



Quantifying the contributions of individual NO_x sources to the trend in ozone radiative forcing

K. Dahlmann*, V. Grewe, M. Ponater, S. Matthes

Deutsches Zentrum für Luft- und Raumfahrt, Institut für Physik der Atmosphäre, Oberpfaffenhofen, Germany

ARTICLE INFO

Article history:

Received 19 October 2010

Received in revised form

28 February 2011

Accepted 28 February 2011

Keywords:

Emission sectors

Road transport

Radiative efficiency

Ozone production efficiency

Air traffic

Climate impact

ABSTRACT

Source attribution of ozone radiative forcing (RF) is a prerequisite for developing adequate emission mitigation strategies with regards to climate impact. Decadal means of ozone fields from transient climate-chemistry simulations (1960–2019) are analysed and the temporal development of ozone RF resulting from individual NO_x sources, e.g. road traffic, industry and air traffic, is investigated. We calculated an ozone production efficiency which is mainly dependent on the altitude of NO_x emission and on the amount of background NO_x with values varying over one order of magnitude. Air traffic and lightning are identified as NO_x sources with a two and five times higher ozone production efficiency, respectively, than ground based sources. Second, radiative efficiency of source attributed ozone (i.e. total induced radiative flux change per column ozone) shows clear dependence on latitudinal structure of the ozone anomaly and, to a lesser extent, to its altitude. Lightning induced ozone shows the highest radiative efficiency because lightning primarily enhances ozone in low latitudes in the mid-troposphere (higher altitudes). Superimposed on these effects, a saturation effect causes a decreasing radiative efficiency with increasing background ozone concentrations. Changes in RF attributed to NO_x induced ozone from 1960 to 2019 are controlled by three factors: changes in emissions, changes in ozone production efficiency and changes in the radiative efficiency. Leading effect is emission increase, but changes in ozone production efficiency increase ozone RF by a factor of three for air traffic, or reduce ozone RF by around 30% for ships. Additionally, changes in the radiative efficiency due to saturation effects change ozone RF by 2–5%.

© 2011 Elsevier Ltd. All rights reserved.

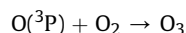
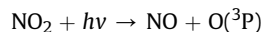
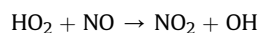
1. Introduction

Ozone changes have the potential to effect climate significantly (e.g. Ramanathan and Dickinson, 1979; Fishman et al., 1979). At the beginning of the 21st century the contribution of tropospheric ozone to anthropogenic radiative forcing (RF) since pre-industrial times was about 0.35 W m⁻² (Forster et al., 2007), making it the third most important greenhouse gas perturbed by human activity, next to carbon dioxide (CO₂) and methane (CH₄).

The global increase of tropospheric ozone abundance has occurred as a consequence of rising anthropogenic emissions of various ozone precursor species (NO_x, CO, CH₄, NMHCs). Numerous studies confirm the major role of increasing NO_x emissions (e.g. Stevenson et al., 2006). However, anthropogenic effects are superimposed on a varying natural background, which may induce trends as well. As anthropogenic and natural trends do not develop independently from each other, unravelling the contributions of

individual sources to the net concentration change and the associated RF is a challenge.

Tropospheric ozone is produced primarily through the reactions:



The impact of NO_x (=NO + NO₂) emissions on the ozone budget has been studied for the total anthropogenic emission, (e.g. Gauss et al., 2006) but also in sector-specific model calculations for, e.g., air traffic (Penner et al., 1999; Grewe et al., 2002; Köhler et al., 2008), shipping (Eyring et al., 2007a), and road traffic (Granier and Brasseur, 2003; Matthes et al., 2007). Most anthropogenic NO_x sources have shown a rapid rise since 1960. Further increases in emissions and thus, in tropospheric ozone are expected in the next decades, though this rate will depend on development of future technologies. By contrast, ozone depletion in the stratosphere since

* Corresponding author.

E-mail address: Katrin.Dahlmann@dlr.de (K. Dahlmann).

1970, due to emission of CFCs, (e.g. WMO, 2003; Dameris et al., 2006), is expected to reverse during the forthcoming decades (Eyring et al., 2007b), which will also impact tropospheric ozone (Grewe, 2007).

In order to evaluate possible attempts to mitigate specific NO_x emissions, systematic knowledge and understanding of the parameters that govern the attributed radiative impact are required.

Early studies, (e.g. Laciš et al., 1990) have shown that the RF produced from a certain amount of ozone depends on the altitude of the perturbation. Ozone increases near the tropopause are radiatively most efficient. As spatial distribution of NO_x emissions from several sources differs, vertical profiles of the resulting ozone changes are very different. Industry, road traffic, and ships mainly emit in the northern mid-latitudes at low altitudes, while lightning emits mainly in the tropical mid to upper troposphere. Therefore ozone induced radiative flux changes (RFC) per unit column change, here defined as the radiative efficiency of an ozone perturbation, will differ significantly between individual NO_x sources. It has not been discussed in previous studies, however, whether and to which extent changes in ozone radiative efficiency have an influence on the temporal development of ozone RF attributed to NO_x emissions.

In this paper we first, quantify the contribution of individual emission sources to the atmospheric ozone concentration, the total climate effect from ozone in terms of their RF, and their radiative efficiency during a 60 year period (1960–2019). Second, we present the variation of chemical and radiative efficiencies of individual NO_x sources. Third, we quantify several non-linear dependencies of the radiative efficiency of individual emission sectors on the ozone background concentrations (Section 5).

Throughout this paper ozone RF will serve as a metric for the impact of ozone on global climate. As Fuglestad et al. (2008) point out, RF is a backward looking measure that describes the radiative impact caused by emissions occurring before the time for which the RF is calculated. It also allows a first order estimate of the global equilibrium surface temperature response via the concept of climate sensitivity (e.g. Dickinson, 1982; Hansen et al., 1997). This makes it particularly useful to intercompare contributions of individual source components where the actual mean surface temperature response cannot be determined due to an insufficient signal to noise ratio.

2. Model description and experimental set up

We applied the fully coupled climate-chemistry model E39/C (Dameris et al., 2005), which consists of the climate model ECHAM4.L39(DLR) (Land et al., 1999) and the chemistry module CHEM (Steil et al., 1998). The latter includes homogeneous and heterogeneous stratospheric reactions, as well as the tropospheric background chemistry CH₄–CO–NO_x–HO_x–O₃. However, NMHC chemistry is omitted, which means that our consideration of individual source contributions is based on NO_x emissions alone. The effect of NMHC chemistry on ozone concentration changes due to, e.g., road traffic and air traffic has been considered in Matthes (2003) and Kentarchos and Roelofs (2002), respectively. The consequences of neglecting NMHC chemistry in our results will be discussed in Section 4.

The employed chemical boundary conditions and emissions for the past and future are complemented in the supplementary material. Here, we only focus on some key issues. Emissions of NO_x are either prescribed (biomass burning, road traffic, ships, soils, industry, and air traffic) or calculated online (lightning, N₂O degradation). The development of individual NO_x emissions from different tropospheric sources from 1960–2019 is presented in

Fig. 1. The growth of anthropogenic NO_x emissions is based on economic scenarios of GDP (gross domestic product) development according to OECD (1997). Industry has contributed the highest NO_x emissions ever since the 1960s and further rapid rise is expected until 2019. The second largest emitter of NO_x has been road traffic, whose contribution in the past (1960–1999) increased proportionally with industry. For future road traffic emissions mitigation measures are taken into account (Supplementary material). NO_x emissions from air traffic rise with a similar rate as those of industry but are only about 2% of industry emissions in absolute numbers (for visualisation purposes, the emissions of air traffic are multiplied by a factor of 10 in Fig. 1a). They are nevertheless considered separately as they occur in sensible regions of the atmosphere and, in contrast to the other transport sectors, are expected to grow in the future. Natural sources, lightning and soils as well as biomass burning, display only a small trend in emissions during the time period considered here. These emissions include a mean seasonal cycle but, except for lightning, without interannual variability.

The model system has been extensively evaluated against measurements within international validation activities, (e.g. Austin et al., 2003; Shine et al., 2003; Brunner et al., 2005), and has been applied for a variety of scientific questions, for example, with regard to the future development of the ozone layer (Schnadt et al., 2002; Dameris et al., 2006) or aviation impacts (Grewe et al., 2002, and references therein).

An ensemble of transient simulations for the recent past (1960–1999) and for the future (2000–2019) is used in order to calculate the time development of ozone change patterns for different sources. For a detailed description of the simulations for the past and for the future see Dameris et al. (2005) and Dameris et al. (2006), respectively.

Essential for the purpose addressed in this paper is the inclusion of a NO_x–ozone tracking diagnostic for individual emission sources in the E39/C simulations (Grewe, 2004) for which all sources for NO_x (lightning, biomass burning, soils, industry, road traffic, ships, air traffic and stratospheric N₂O degradation) are specified separately. To each of these 8 sources a NO_y tracer is assigned in addition to the chemical species in the module CHEM, which receives the individual emission and an individual NO_y loss proportional to the total NO_y loss. Each NO_y tracer is associated with an ozone tracer, which experiences an ozone production proportional to the ratio of specific NO_y to total NO_y concentration multiplied by the total ozone production via the reaction of NO + HO₂ → NO₂ + OH. A further ozone tracer is included to account for ozone production by O₂ photolysis (mainly in the stratosphere). Grewe (2004) and Grewe et al. (2010) compared two approaches to calculate the contribution of NO_x emissions to ozone: 1) the “tagging” method, as

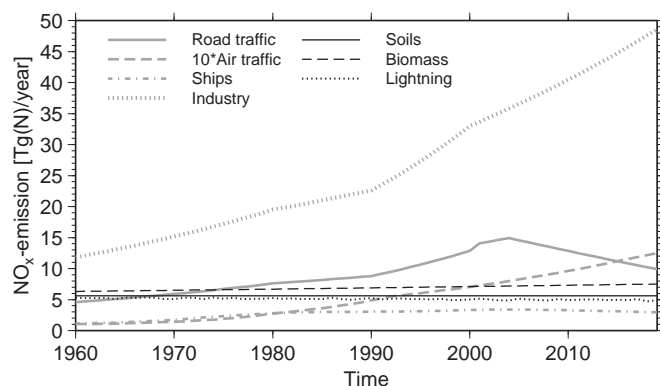


Fig. 1. Trends in NO_x emission of different sources in Tg(N)/a from 1960 to 2019.

described above and 2) calculation of individual ozone perturbations by dedicated simulations for each individual NO_x emission (sensitivity method). The latter approach has problems to correctly represent an individual ozone contribution in the framework of various competing component emissions, due to non-linearities in the chemistry. Significant differences to the conceptually superior tagging approach occur mainly in the tropopause region. However, both approaches produce similar ozone trends (Grewe, 2004).

RF and RFC calculations are based on mean annual cycles of ozone distributions simulated by the CCM, averaged over individual decades (1960–1969, 1970–1979, etc.). The RFC of the ozone change pattern from each individual emission source is obtained in dedicated model calculations (over one year, with three months spinup) by subtracting the contribution of the individual source from the complete ozone field for each time slice. We calculate the RF and RFC values according to the "fixed dynamical heating" concept, (e.g. Ramanathan and Dickinson, 1979; Ramaswamy et al., 2001). This method has been adopted for use in ECHAM4 as described in Stuber et al. (2001). The ECHAM4 radiation scheme performs well for tropospheric ozone but shows a tendency to underestimate

the ozone RF for stratospheric perturbations (Forster et al., 2001). Stuber et al. (2001, 2005) give examples for realistic and idealised ozone perturbations calculated with this method.

Key to this paper is a qualification of the component RF contributed by each individual NO_x source. Commonly, RF is determined relative to the pre-industrial state, but it may also be used to compare the changes between any two points in time (Fuglestedt et al., 2010). In this sense it can be calculated to quantify the changes from anthropogenic contributions as well as from natural contributions (like solar radiative input to the climate system, e.g. Forster et al. (2007)). In our case, as we use simulations starting at 1960, the ozone RF contributions from individual NO_x sources are calculated as changes in RFC with respect to 1960 conditions:

$$\text{RF}^t = \text{RFC}^t - \text{RFC}^{1960} \quad (1)$$

However, while RF values are given relative to the 1960 decade, radiative efficiencies are calculated as the ratio between the total RFC induced by an individual ozone component and the ozone

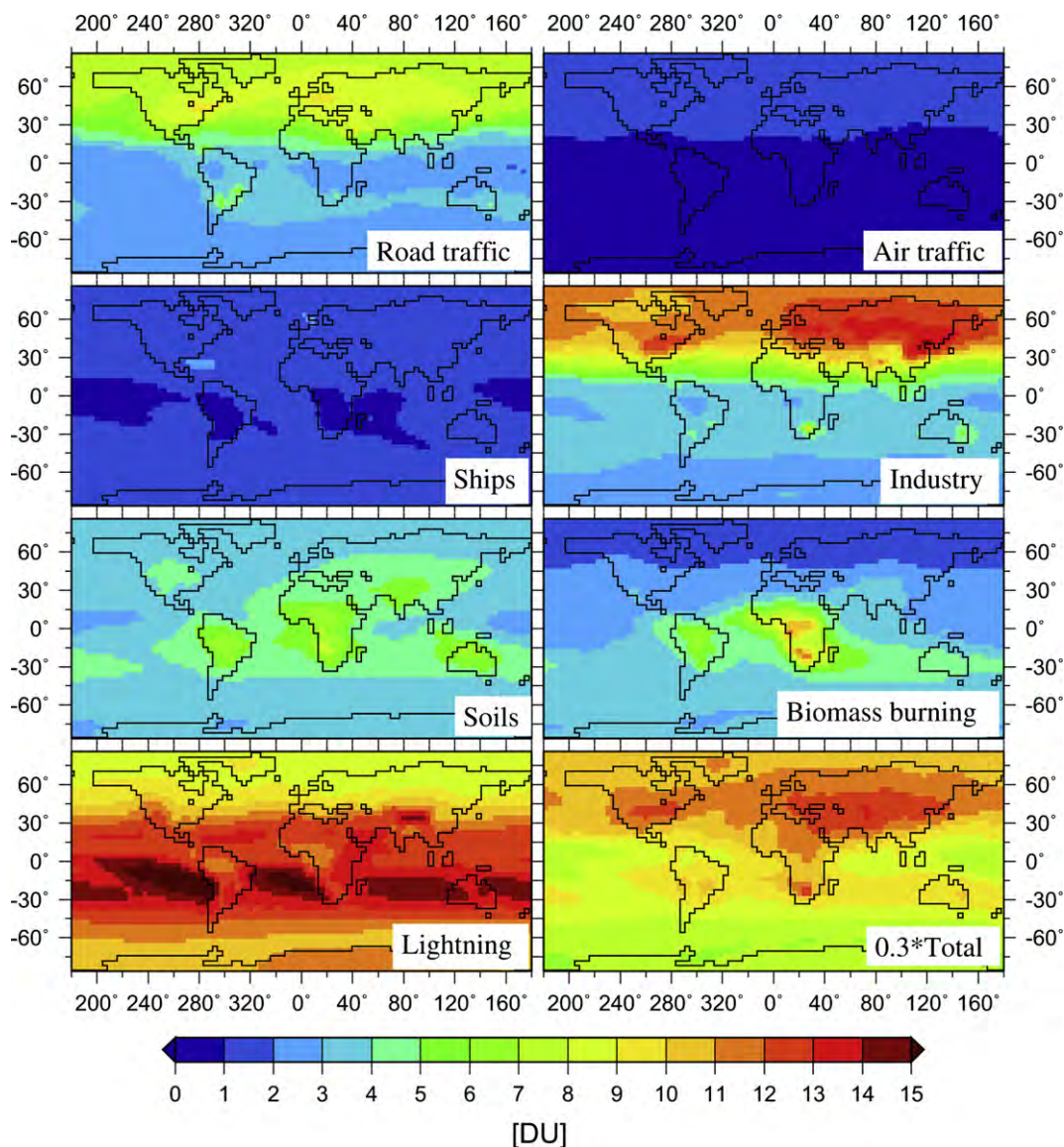


Fig. 2. Contribution from different sources to decadal mean ozone column during the 1990s in DU. For a better visibility the sum of all tropospheric sources (Total) is multiplied with a factor of 0.3.

column of this component. By analysing temporal developments of both quantities, it is possible to interpret differences of the radiative efficiency between different sources as well as the change of radiative efficiency of a given source over time. A similar method has been used before to describe the radiative efficiency of ozone at different latitudes (e.g. Mickley et al., 1999), but not for characterising the contributions of different emission sources.

3. Trends in ozone and ozone RF

3.1. Ozone

Global contribution to column ozone from tropospheric sources during the 1990s is presented in Fig. 2. Anthropogenic sources like road traffic, air traffic, ships, and industry induce higher ozone columns in the northern than in the southern hemisphere due to higher NO_x emissions in the northern hemisphere. Although NO_x emissions of road traffic and industry take place over land only, ozone column over oceans is also affected because of long-range transport of NO_x and ozone. The ozone column contribution from soils shows a broad maximum between about 60°N and 30°S . NO_x emissions from biomass burning induce a characteristic double maximum of ozone change of Central and South Africa due to natural and anthropogenic fires in the rainforest.

Lightning primarily occurs in tropical regions with deep convection. As in those regions the HNO_3 wash-out is also most effective, the highest ozone columns for lightning can be found rather in the outflow regions of main convective activity: Lightning NO_x is transported downwind from convective regions into regions with large-scale subsidence characterised by clear-sky conditions and high UV radiance, leading to pronounced ozone column maxima, e.g. off the east coast of Africa and South America. This

model result is consistent with aircraft measurements of high NO_x levels in the outflow of mesoscale convection systems (Huntrieser et al., 2007).

Fig. 3a shows the trend in global mean column ozone between 1960 and 2019 for individual tropospheric NO_x sources. Although global mean NO_x emissions by lightning are of similar magnitude as those from biomass burning or soils, its contribution to total ozone column is about three times larger. A similar excess can be found for air traffic: While NO_x emissions of air traffic represent only 30% of ship NO_x emissions, the ozone column of air traffic and ships in the 2000s is of comparable magnitude. We explain this feature in terms of differences in the ozone production efficiency, which indicates how many ozone molecules are produced per molecule NO_x (Fig. 3b). Ozone production efficiency is much higher for lightning and air traffic (100 and 50 molecules O_3 per molecule NO_x respectively) than it is for ground based sources (between 10 and 30 molecules O_3 per molecule NO_x). While lightning produces about 100 molecules O_3 per molecule NO_x , air traffic produces about 50 and the other sources between 10 and 30 molecules O_3 per molecule NO_x . The reason for a higher ozone production efficiency of lightning and air traffic is the higher amount of UV radiance at higher altitudes, lower background concentration of NO_x and the longer lifetime of ozone.

Differences in ozone production efficiency among various ground based sources are caused by the strong dependency of ozone production efficiency on background NO_x ($\text{NO}_x = \text{NO}_x + \text{NO}_3 + \text{N}_2\text{O}_5 + \text{HNO}_4$). The ozone production rate at low background NO_x levels is very small and increases very fast with increasing concentrations (e.g. Grooß et al., 1998). If a certain amount of NO_x is exceeded, further increase of NO_x causes a decrease of ozone production efficiency (saturation effect) and, eventually, even ozone depletion. Thus emissions in polluted areas (e.g. Europe) have a lower ozone production efficiency than in remote areas (e.g. South Africa) (Fig. 4). The same relation explains the strong increase of the ozone production efficiency of air traffic from 1960–1980: In the 1960s a very low background NO_x of less than 0.3 ppbv NO_x at cruise altitudes limits ozone production by aviation emissions, while the higher background level in the 1990s causes an increasing ozone production (Fig. 4, net O_3 -production rate of 250 hPa multiplied with 10). Ozone production efficiency of

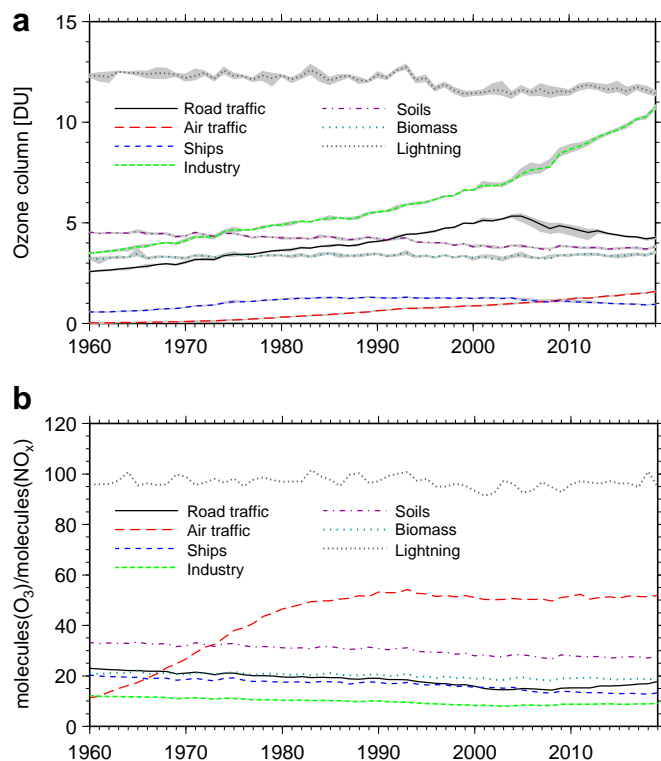


Fig. 3. Trends between 1960 and 2019 of (a) global mean ozone column in DU and (b) ozone production efficiency in molecules(O_3)/molecule(NO_x) for different sources. Grey shaded areas represent spread between ensemble simulations (a).

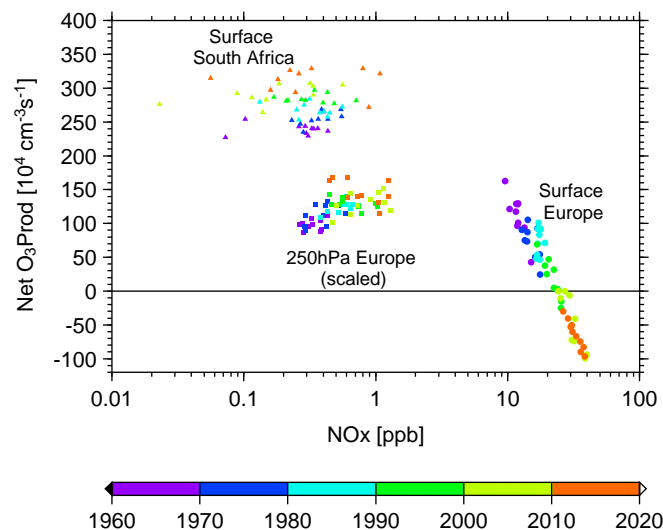


Fig. 4. Net O_3 -production rate as function of background NO_x calculated by E39/C for summer for three different regions: surface South Africa (triangles), surface Europe (circles) and 250 hPa Europe (squares, net O_3 -production rate multiplied with 10). Time is indicated by colours.

industry is lower than that of other ground based sources because industry emits in already polluted areas (about 20 ppbv NO_x) where increasing NO_x values cause decreasing ozone production efficiency. Soils and biomass burning on the other hand emit mainly in remote areas with background NO_x between 0.1 ppbv and 1 ppbv. The ozone production efficiency of soil NO_x emissions is higher in comparison to emissions from biomass burning, because soil emissions peak in the northern midlatitude summer (fertilisation in agricultural regions), when ozone production is enhanced.

Fig. 3b further shows that ozone production efficiency of surface sources, except road traffic, decreases with time, consistent with what has been shown in Lamarque et al. (2005), who analysed total ozone burden. This is caused by an overall increase in NO_x concentrations, leading to the above mentioned saturation effect for each of the individual contributions. An exception is the ozone production efficiency of road traffic which shows a little increase since 2005. The reason for this is the assumed future scenario implying that NO_x emissions of road traffic only increase in non-industrial (remote) regions but decrease in industrial (polluted) regions beyond 2005 (see Fig. 2 of Supplementary material). This is consistent with satellite measurements of Uno et al. (2007) and Konovalov et al. (2008), which show increasing NO_x emissions over Eastern Asia and decreasing NO_x emissions over Western and Central Europe, respectively.

3.2. Radiative forcing

Fig. 5a shows the ozone RF caused by individual NO_x sources discussed in the last section. As we display RF with respect to 1960, the quite different absolute magnitude of the individual ozone contributions (Fig. 3a) is no longer apparent in the RF values but can be seen in Table 1 of the supplementary material. However, temporal correlation between RF change and ozone column change is high for each component. Industry and road traffic for example

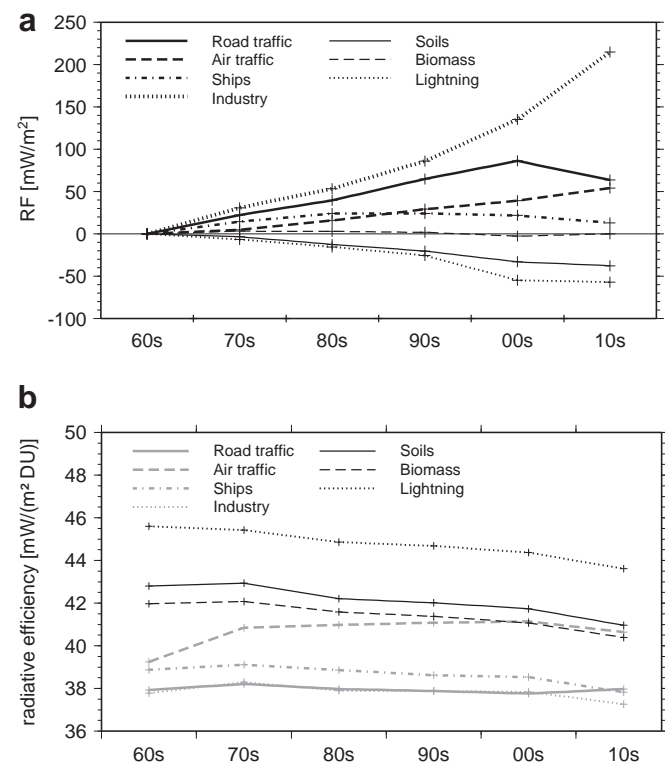


Fig. 5. a) Changes of global mean ozone RF in mW m^{-2} with respect to 1960s and b) trends in global mean ozone radiative efficiency for different sources in $\text{mW}/(\text{m}^2\text{DU})$.

show the highest ozone column change as well as highest RF. Negative values displayed in Fig. 5a represent a reduced warming compared to 1960.

In order to quantify differences in specific radiative impact of an individual ozone pattern we display in Fig. 5b the radiative efficiency as defined in section 2. Respective values range between 38 and 46 $\text{mW}/(\text{m}^2\text{DU})$.

For the tropospheric sources, Fig. 5b demonstrates that the variation over time of the radiative efficiency of individual source contributions is less than the source to source difference for a given time. The difference in net radiative efficiency is mainly controlled by the longwave forcing (greenhouse effect). Due to the dependency of the greenhouse effect on the temperature of the absorber the radiative efficiency is larger for ozone changes near the tropopause (Lacis et al., 1990). Beside the altitude dependency there is a latitude dependency (Fig. 6): The same temperature difference produces a larger greenhouse effect at higher temperatures due to the non-linear T^4 dependency of the longwave emission. Fig. 6 shows that the radiative efficiency at low latitudes (about 50 $\text{mW}/(\text{m}^2\text{DU})$) is almost three times higher than at high latitudes (about 15 $\text{mW}/(\text{m}^2\text{DU})$), confirming earlier results of Berntsen et al. (1997). The altitude dependency remains visible: Lightning and air traffic have a somewhat higher radiative efficiency than the ground based sources. However, while the difference of radiative efficiency between equator and pole is about 30 $\text{mW}/(\text{m}^2\text{DU})$, the difference of radiative efficiency between ground based sources and sources in higher altitudes is only up to 10 $\text{mW}/(\text{m}^2\text{DU})$. The radiative efficiency of lightning ozone is highest because the altitude effect and the latitude effect are working in the same direction. Aircraft emissions have an intermediate radiative efficiency since the emissions take place at higher altitudes but in mid and high latitudes. The radiative efficiency of soils and biomass burning exceeds that of road traffic, ships and industry since those emissions take place mainly in tropical regions. Radiative efficiency of individual emissions also changes over time. For all but air and road traffic the radiative efficiency decreases due to saturation effects which we will further analyse in Section 5.

Explaining the temporal development of RF of the individual emission sources in Fig. 5a is straightforward. As RF is the change in RFC with respect to 1960, the time development of ozone RF is given by the time development of RFC. We split the percentual changes in RFC into three relative terms: change in NO_x emission (E), ozone mass per NO_x emission (O_3/E , chemistry) and radiative efficiency (RFC/O_3 , radiation) between 1960s and 2010s:

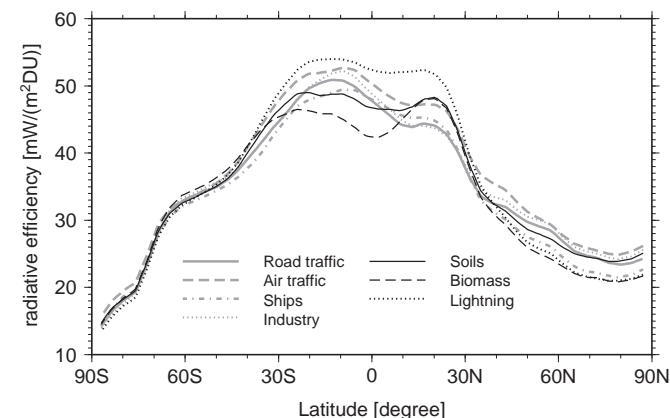


Fig. 6. Zonal mean of ozone radiative efficiency for different sources for 2010–2019 in $\text{mW}/(\text{m}^2\text{DU})$.

$$\frac{\text{RFC}^{2010}}{\text{RFC}^{1960}} = \frac{E^{2010}}{E^{1960}} \times \frac{\frac{O_3^{2010}}{E^{2010}}}{\frac{O_3^{1960}}{E^{1960}}} \times \frac{\text{RFC}^{2010}}{\frac{\text{RFC}^{1960}}{O_3^{1960}}} \quad (2)$$

The temporal development of these terms for industry, soils and air traffic is displayed in Fig. 7. Industry provides a NO_x emission rise by more than a factor three in 2010 compared to 1960. As the ozone production efficiency of industry decreases in the same time by 25%, the resulting RFC in 2010 is only a factor 2.5 higher than in 1960 (Fig. 7a). A similar effect is evident for soil emissions (Fig. 7b). Although emissions stay constant over the period considered here, the RFC decreases between 1960 and 2010 by 19% due to reduced ozone production (−16%) and radiative efficiencies (−4%). In contrast, the RFC change of air traffic is higher (30-fold) than the change in emissions (tenfold) (Fig. 7c), due to increase of ozone production (+196%) and radiative efficiency (+4%).

The split of RFC change into these three terms for all emission sources is displayed in Fig. 8. The trend in ozone RF from lightning emissions is negative: Emissions decrease by 6% because convective activity becomes less despite of stronger individual events (Grewe, 2009) and radiative efficiency decreases by 5%. As for industry, the ozone RFCs of road traffic and shipping grow more slowly than the emissions due to decreasing specific ozone production (−27 and −32%) and radiative efficiency (−1 and −4%). The RF trend for biomass burning is close to zero because the increasing emissions (16%) are compensated by chemical (−14%) as well as radiative (−4%) saturation effects.

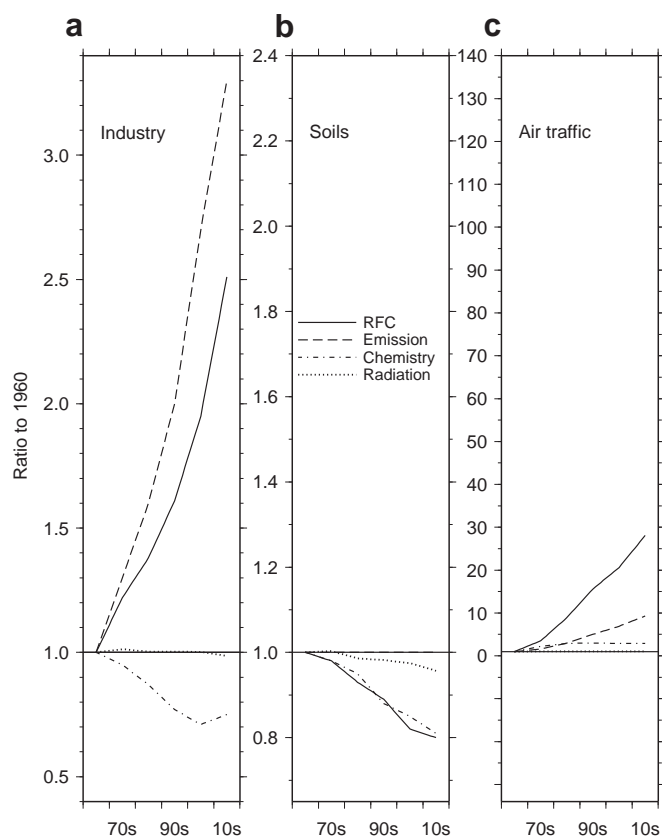


Fig. 7. Temporal development of ozone RF relative change (solid) caused by changes of NO_x emissions (dashed), ozone production per NO_x emission (dashed-dotted) and radiative efficiency (dotted) for a) industry, b) soils and c) air traffic emissions. Vertical axes are adopted according to absolute values of RF changes.

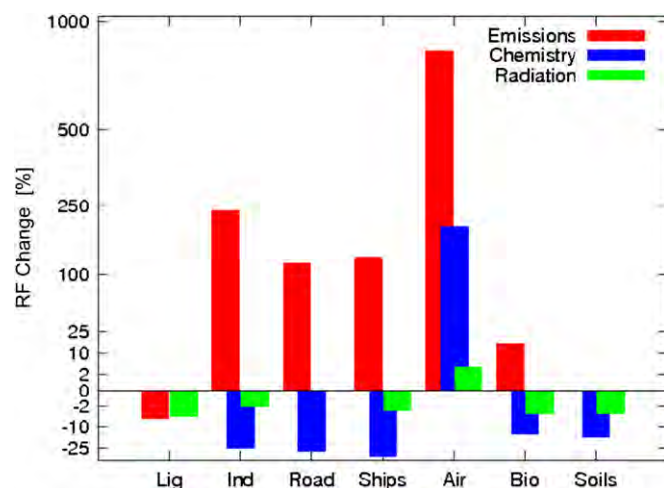


Fig. 8. Percentage changes in ozone RF from 1960s to 2010s due to changes of NO_x emissions (light grey), ozone production per NO_x emission (dark grey) and radiative efficiency (black) for lightning (Lig), industry (Ind), road traffic (Road), ships (Ships), air traffic (Air), biomass burning (Bio), and soil (Soils) emissions. The chemistry effect of lightning and the radiation effect of road traffic are too small to be visible.

4. Uncertainty discussion

Our analysis is based on the calculation of ozone distributions with the online tagging mechanism. As discussed in Section 2 (and elsewhere, e.g. Wang et al. (2009) and explicitly shown by Grewe et al. (2010)), tagging is the only appropriate method for source attribution. The tagging method may lead to enhanced changes in the upper troposphere and lower stratosphere by numerical diffusion (Grewe, 2004), but the excess remains small compared to the background field. However, due to the high radiative efficiency of ozone perturbations around the tropopause, the impact on RF is approximately 10%, as estimated from an idealised ozone perturbation of 30 DU around the tropopause giving 1 W m⁻² RF (Stuber et al., 2005).

The CCM we use (E39/C) includes a background NO_x–HO_x–CO–CH₄ chemistry scheme for free and upper tropospheric chemical conditions. NMHC emissions (which are not considered in E39/C) have the potential to enhance long-range transport of nitrogen compounds via formation of additional PAN (Matthes et al., 2007), thus allowing additional ozone production also in remote regions. Working in the other direction, an increase in HO_x due to NMHC chemistry decreases the lifetime of ozone. The net effect of the NMHC absence in the simulations presented in this paper is sector dependent: For the air traffic contribution it may yield an underestimation of the resulting ozone change of about 10% (Kentarchos and Roelofs, 2002). NMHC chemistry is more important for surface based emission sources. Assessing road traffic induced ozone increase from NO_x emissions alone captures around 70% of total ozone impact of road traffic (Matthes et al., 2007). To analyse the ozone perturbation deficits resulting from missing NMHC chemistry in E39/C we performed an additional simulation with a similar calculation method as Hoor et al. (2009). In this simulation we used 1990s conditions but with road traffic NO_x emissions turned off. The resulting zonal mean ozone perturbation is shown in Fig. 9. The pattern of ozone perturbation as well as the absolute values are comparable with those from Fig. 6 from Hoor et al. (2009) scaled to 100%. This shows that E39/C produces reasonable ozone perturbations results despite missing NMHC chemistry. The RF since pre-industrial times of this ozone perturbation is 31.1 mW m⁻², which compares well with 27.9 mW m⁻² yielded in Hoor et al. (2009) as the mean of a variety of models including NMHC chemistry.

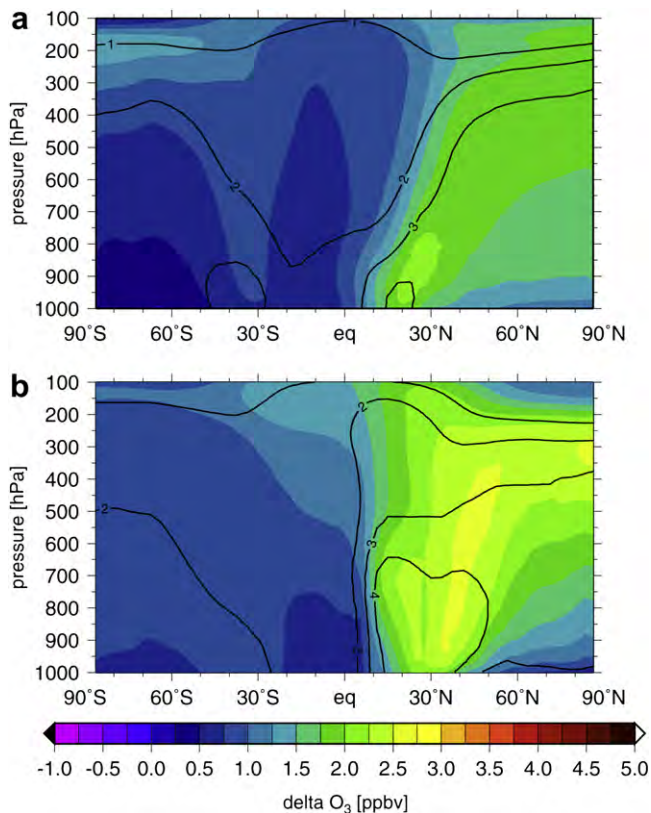


Fig. 9. Zonal mean ozone perturbation from road traffic for an additional simulation for January (a) and July (b), respectively. Solid contours show the changes relative to total ozone concentration in percent.

The IPCC estimate of anthropogenic tropospheric ozone forcing since pre-industrial times is 0.35 W m^{-2} with an uncertainty range of $0.25\text{--}0.65 \text{ W m}^{-2}$ (Forster et al., 2007), values referring to all anthropogenic precursor emissions that have occurred between 1750 and 2005, under the assumption of zero anthropogenic emissions in 1750 and biomass burning sources reduced by 90% for 1750. To assess whether our RFs (Fig. 5a) are consistent with IPCC values we have calculated the RFC difference between the case of anthropogenic NO_x emissions (industry, ship, road and air traffic) for the decade preceding 2000 and the case of no anthropogenic NO_x emissions. This deviates from our standard RF definition (relative to 1960) but can be assumed to represent the RF since the pre-industrial era. In addition, we consider 90% of the biomass burning emissions and the respective RFC to be of anthropogenic origin. With this approach we yield a tropospheric ozone RFC of 0.64 W m^{-2} for the decade preceding 2000, a value at the upper boundary of the IPCC uncertainty range.

For some individual sectors our method yields component RFs that are within the range of other modelling studies, e.g., for lightning (Toumi et al., 1996), aircraft (Sausen et al., 1999; Fuglestedt et al., 2008), and ship emissions (Fuglestedt et al., 2008). With respect to biomass burning, the absolute emission strength has varied largely among other studies. Scaling results given by Unger et al. (2008) to a similar emission strength that we use leads to a differences between the respective RFs slightly lower than 25%. As for road traffic we prescribe larger emissions compared to, e.g., Fuglestedt et al. (2008) but the corresponding radiative efficiency is nevertheless similar: They estimated (see their Supplementary materials) 25 molecules ozone production per emitted NO_x molecule and $45 \text{ mW}/(\text{m}^2\text{DU})$ radiative efficiency, which compares well with our results (Figs. 3b and 5b).

5. Non-linearities of radiative efficiency

5.1. Saturation effects

Radiative efficiency generally decreases over time, particularly after 1980 (Fig. 5b). By the 2010s the radiative efficiency of most source contributions is about 2–3% lower than during the 1980s, except for the air traffic and road traffic components. In this section we present and discuss results of dedicated RFC calculations performed in order to quantify a potential saturation effect in the radiative efficiency dependent on the background ozone level.

To this end, the radiative efficiency of the ozone change induced by all tropospheric sources for the 1990s was calculated with the background ozone gradually increasing. Six different radiative efficiencies were calculated using an ozone background amplified by factors of one, two, three, four, five and six. The results are displayed in Fig. 10. The higher the background ozone is, the lower the resulting radiative efficiency. This effect is much more pronounced for the longwave forcing than for the shortwave forcing, because ozone absorbs longwave radiation only in a limited number of relatively narrow spectral bands, which may get saturated much faster than the wider absorption band in the solar spectral range.

5.2. Additivity

We now consider to which extend the non-linear saturation effect, as discussed above, limits the additivity of the RF of a number of different components. Due to the saturation effect the impact of each individual contribution to the RF budget depends on the assumed background ozone. Commonly the RF of a specific emission is calculated either by the difference between RFC with and RFC without this emission or between RFC with emission and RFC with doubling of this emission. In both cases the ozone background is inadequately high as the ozone produced by all other sources is included in the background concentration. Due to the saturation effect discussed in Section 5.1 this will lead to a low biased RF.

We performed a sensitivity simulation, in which the RFC induced by the sum of all ozone perturbations from tropospheric sources is calculated. The RFC of the whole ozone field is compared with the sum of all separately calculated components as presented in Section 3.2. As in the previous subsection the comparison uses 1990s conditions as an example. In Fig. 11 the longwave, shortwave and net RFC for both calculation methods are shown. While the shortwave forcing of tropospheric sources doesn't show any

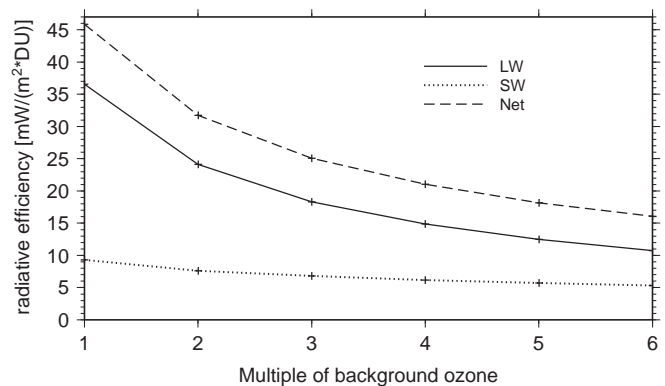


Fig. 10. Dependency of ozone radiative efficiency in $\text{mW}/(\text{m}^2\text{DU})$ of tropospheric sources on background ozone in units of absolute ozone fields of the 1990s. LW (solid), SW (dotted) and Net radiative efficiency (dashed) are presented separately.

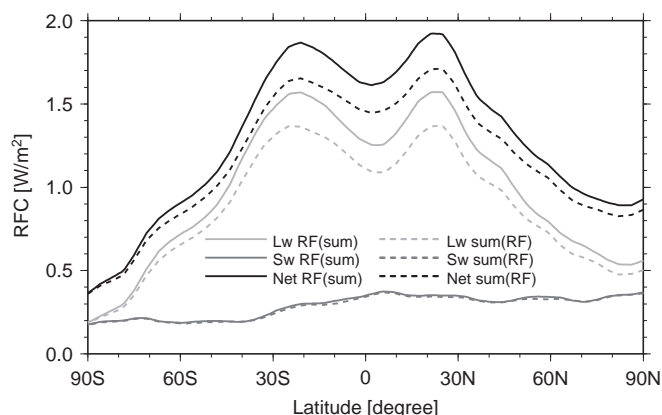


Fig. 11. Non-linearity of the zonal mean RFC of tropospheric sources. LW RFC (light grey), SW RFC (dark grey) and Net RFC (black) for the RFC calculation of the sum of disturbance (solid) and the sum of separately calculated RFC (dashed).

substantial deviation from perfect additivity, the longwave forcing of the sum of separately calculated RFC is about 0.15 W m^{-2} , i.e. 10%, lower than the RFC of the sum of ozone changes. The same conclusion holds for the relation between the net RF of the sum of individual ozone change pattern and the sum of the individually calculated RFs. Hence, 10% may be taken as a typical value for the underestimation yielded if the ozone RF for a combination of sources is determined by simply summing up the component RFs.

6. Conclusions

We separate three factors which govern changes in ozone RF for different sectors and during the period 1960–2019: (1) variation of NO_x emission, (2) ozone production efficiency and (3) radiative efficiency. We show that the ozone production efficiency (ozone production per molecule NO_x) and therewith the induced ozone column change strongly varies between different emission sources due to emission altitude and background NO_x level. Ozone production efficiencies of lightning and industry emissions differ by one order of magnitude. The dependency on the background NO_x level is significant, e.g., for industry and soils. Soil emission occurs in remote areas of relatively low background concentration and produces about three times more ozone per emitted NO_x molecule than industry, which emits in polluted areas.

The attributed RF of tropospheric sources in general shows a strong correlation with ozone column change: A high (low) ozone column causes a large (weak) RF. However, we found that this straightforward relation is modified by non-negligible effects, which can be explained in terms of radiative efficiency (RFC per DU ozone change). We analyse the dependence on emission latitude and altitude for individual sectors. The effect of emission latitude is about three times larger than the effect of emission altitude.

Additional to the modulating impact of the latitudinal and vertical structure of the ozone perturbation pattern on the induced radiative efficiency, we find a saturation effect which causes a decreasing radiative efficiency with increasing background ozone due to saturation of absorption bands. This saturation effect also causes a deviation from perfect additivity when individual RF contributions are considered.

Summarising, the results indicate that the temporal development of ozone RF related to traffic and industry from 1960 to 2019 is mainly controlled by changes in emissions, leading to a significant increase of ozone RF. Nevertheless, radiative impact of NO_x emission sources is also controlled by changes in ozone production efficiency and radiative efficiency. For example ozone production

efficiency of air traffic increases by a factor of three but decreases by around 30% for ships due to those effects.

The knowledge of attributed ozone production and radiative efficiencies for individual NO_x emission sources is important for comparison of different emissions sources, e.g., for mitigation strategies. As both ozone production and radiative efficiency of air traffic are higher than those of industry, a shift (e.g. trading) of NO_x emission from industry to air traffic, for example, would increase the total radiative impact of the same amount of NO_x emissions.

Acknowledgements

This work has been supported by the Integrated Project QUANTIFY and the Network of Excellence ECATS of the EU 6th Framework Programme.

Appendix. Supplementary material

Supplementary data related to this article can be found online at [doi:10.1016/j.atmosenv.2011.02.071](https://doi.org/10.1016/j.atmosenv.2011.02.071).

References

- Austin, J., Shindell, D., Beagley, S., Brühl, C., Dameris, M., et al., 2003. Uncertainties and assessments of chemistry-climate models of the stratosphere. *Atmos. Chem. Phys.* 3, 1–27.
- Berntsen, T., Isaksen, I., Myhre, G., Fuglestedt, J., Stordal, F., et al., 1997. Effects of anthropogenic emissions on tropospheric ozone and its radiative forcing. *J. Geophys. Res.* 102 (D23), 28101–28126.
- Brunner, D., Staehelin, J., Roger, H., Köhler, M., Pyle, J., et al., 2005. An evaluation of the performance of chemistry transport models - part 2: detailed comparison with two selected campaigns. *Atmos. Chem. Phys.* 5, 107–129.
- Dameris, M., Grewe, V., Ponater, M., Eyring, V., Mager, V., et al., 2005. Longterm changes in a transient simulation employing an interactively coupled chemistry-climate model under realistic forcings. *Atmos. Chem. Phys.* 5, 2121–2145.
- Dameris, M., Matthes, S., Deckert, R., Grewe, V., Ponater, M., 2006. Solar cycle effect delays onset of ozone recovery. *Geophys. Res. Lett.* 33, L03806.
- Dickinson, R., 1982. Modelling climate changes due to carbon dioxide increases. In: Clerk, W.C. (Ed.), *Carbon Dioxide Review*. Oxford University Press, New York, pp. 101–133.
- Eyring, V., Stevenson, D., Lauer, A., Dentener, F., Butler, T., et al., 2007a. Multi-model simulations of the impact of international shipping on atmospheric chemistry and climate in 2000 and 2030. *Atmos. Chem. Phys.* 7, 757–780.
- Eyring, V., Waugh, D., Bodeker, G., Cordero, E., Akiyoshi, H., et al., 2007b. Multi-model projections of stratospheric ozone in the 21st century. *J. Geophys. Res.* 112, D16303.
- Fishman, J., Solomon, S., Crutzen, P., 1979. Observational and theoretical evidence in support of tropospheric ozone. *Tellus* 31, 432–446.
- Forster, P., Ponater, M., Zhong, W.-Y., 2001. Testing broadband radiation schemes for their ability to calculate the radiative forcing and temperature response to stratospheric water vapour and ozone changes. *Meteorol. Z.* 10 (5), 387–393.
- Forster, P., Ramaswamy, V., Artaxo, P., Bernsten, T., Betts, R., et al., 2007. Changes in atmospheric constituents and in radiative forcing. In: Solomon, S., Qin, D., Manning, M., Chen, Z., Marquis, M., et al. (Eds.), *Climate Change 2007: The Physical Science Basis. Contribution of Working Group I to the Fourth Assessment Report of the Intergovernmental Panel on Climate Change*. Cambridge University Press, Cambridge, United Kingdom and New York, NY, USA.
- Fuglestedt, J., Bernsten, T., Myhre, G., Rypdal, K., Skeie, R., 2008. Climate forcing from the transport sectors. *PNAS* 105, 454–458.
- Fuglestedt, J., Shine, K., Bernsten, T., Cook, J., Lee, D., Stenke, A., Skeie, R., Velders, G., Waitz, I., 2010. Transport impacts on atmosphere and climate: Metrics. *Atmos. Environ.* 44 (37), 4648–4677.
- Gauss, M., Myhre, G., Isaksen, I., Grewe, V., Pitari, G., et al., 2006. Radiative forcing since preindustrial times due to ozone changes in the troposphere and the lower stratosphere. *Atmos. Chem. Phys.* 6, 575–599.
- Granier, C., Brasseur, G., 2003. The impact of road traffic on global tropospheric ozone. *Geophys. Res. Lett.* 30, 1086. doi:10.1029/2002GL015972.
- Grewe, V., 2004. Technical note: a diagnostic for ozone contributions of various NO_x emissions in multi-decadal chemistry-climate model simulations. *Atmos. Chem. Phys.* 6, 1495–1511.
- Grewe, V., 2007. Impact of climate variability on tropospheric ozone. *Sci. Total Environ.* 374, 167–181.
- Grewe, V., 2009. Impact of lightning on air chemistry and climate. In: Betz, H.D., Schumann, U., Laroche, P. (Eds.), *Lightning: Principles, Instruments and Applications of Modern Lightning Research*. Springer Verlag, pp. 524–551.
- Grewe, V., Dameris, M., Fichter, C., Sausen, R., 2002. Impact of aircraft NO_x emissions, part 1: interactively coupled climate-chemistry simulations and

- sensitivities to climate-chemistry feedback, lightning and model resolution. *Meteorol. Z.* 3, 177–186.
- Grewe, V., Tsati, E., Hoor, P., 2010. On the attribution of contributions of atmospheric trace gases to emissions in atmospheric model applications. *Geosci. Model. Dev.* 3, 487–499.
- Grooß, J.-U., Brühl, C., Peter, T., 1998. Impact of aircraft emissions on tropospheric and stratospheric ozone. Part I: chemistry and 2-D Model results. *Atmos. Environ.* 32 (18), 3152–3184.
- Hansen, J., Sato, M., Ruedy, R., 1997. Radiative forcing and climate response. *J. Geophys. Res.* 102, 6831–6864.
- Hoor, P., Borken-Kleefeld, J., Caro, D., Dessens, O., Endresen, O., et al., 2009. The impact of traffic emissions on atmospheric ozone and OH: results from quantify. *Atmos. Chem. Phys.* 9, 3113–3136.
- Huntrieser, H., Schlager, H., Roiger, A., Lichtenstern, M., Schumann, U., et al., 2007. Lightning-produced NO_x over Brazil during TROCCINOX: airborne measurements in tropical and subtropical thunderstorms and the importance of mesoscale convective systems. *Atmos. Chem. Phys.* 7, 2987–3013.
- Kentarchos, A., Roelofs, G., 2002. Impact of aircraft NO_x emissions on tropospheric ozone calculated with a chemistry-general circulation model: sensitivity to higher hydrocarbon chemistry. *J. Geophys. Res.* 107 (D13), 4175.
- Köhler, M., Rädcl, G., Dessens, O., Shine, K., Rogers, H., et al., 2008. Impact of perturbations to nitrogen oxide emissions from global aviation. *J. Geophys. Res.* 113, D11305.
- Konovalov, I., Beekmann, M., Burrows, J., Richter, A., 2008. Satellite measurement based estimates of decadal changes in European nitrogen oxides emissions. *Atmos. Chem. Phys.* 8 (10), 2623–2641.
- Lacis, A., Wuebbles, D., Logen, J., 1990. Radiative forcing of climate by changes in vertical distribution of ozone. *J. Geophys. Res.* 95, 9971–9981.
- Lamarque, J., Hess, P., Emmons, L., Buja, L., Washington, W., Granier, C., 2005. Tropospheric ozone evolution between 1890 and 1990. *J. Geophys. Res.* 110 (D08304).
- Land, C., Ponater, M., Sausen, R., Roeckner, E., 1999. The ECHAM4.L39/DLR Atmosphere GCM - Technical Description and Model Climatology DLR Forschungsbericht 1999-31, Köln, ISSN 1434–8454.
- Matthes, S., 2003. Globale Auswirkung des Straßenverkehrs auf die chemische Zusammensetzung der Atmosphäre. Ph.D. thesis, DLR-Forschungsbericht.
- Matthes, S., Grewe, V., Sausen, R., Roelofs, G.-J., 2007. Global impact of road traffic emissions on tropospheric ozone. *Atmos. Chem. Phys.* 7, 1707–1718.
- Mickley, L., Murti, P., Jacob, D., Logan, J., Koch, D., Rind, D., 1999. Radiative forcing from tropospheric ozone calculated with a unified chemistry-climate model. *J. Geophys. Res.* 104, 30153–30172.
- OECD, 1997. Globalisation and linkages: macro-structural challenges and opportunities. In: Richardson, P. (Ed.), OECD Economic Studies. Organisation for Economic Co-operation and Development.
- Penner, J., Lister, D., Griggs, D., Dokken, D., McFarland, M.E., 1999. Aviation and the Global Atmosphere; a Special Report of IPCC Working Groups I and III. Intergovernmental Panel on Climate Change. Tech. Rep. Cambridge University Press, Cambridge, UK and New York, NY, USA, pp. 365.
- Ramanathan, V., Dickinson, R., 1979. The role of stratospheric ozone in the zonal and seasonal radiative energy balance of the earth-troposphere system. *J. Atmos. Sci.* 36, 1084–1104.
- Ramaswamy, V., Boucher, O., Haigh, J., Hauglustaine, D., Haywood, J., et al., 2001. Radiative forcing of climate change. In: Joos, F., Srinivasan, J. (Eds.), *Climate Change 2001: The Scientific Basis*. Contribution of Working Group I to the Third Assessment Report of the Intergovernmental Panel on Climate Change. Cambridge University Press, Cambridge, United Kingdom and New York, NY, USA.
- Sausen, R., Isaksen, I., Hauglustaine, D., Grewe, V., Lee, D.S., et al., 1999. 2005. Aviation radiative forcing in 2000: an update on IPCC. *Meteorol. Z.* 14, 555–561.
- Schnadt, C., Dameris, M., Ponater, M., Hein, R., Grewe, V., Steil, B., 2002. Interaction of atmospheric chemistry and climate and its impact on stratospheric ozone. *Clim. Dyn.* 18, 501–517.
- Shine, K., Bourqui, M., Forster, P., Hare, S., Langematz, U., et al., 2003. A comparison of model-predicted trends in stratospheric temperatures. *Q. J. R. Meteor. Soc.* 129, 1565–1588.
- Steil, B., Dameris, M., Brühl, C., Crutzen, P., Grewe, V., et al., 1998. Development of a chemistry module for GCMs: first results of a multiannual integration. *Ann. Geophys.* 16, 205–288.
- Stevenson, D., Dentener, F., Schultz, M., Ellingsen, K., van Noije, T., et al., 2006. Multimodel ensemble simulations of present-day and near-future tropospheric ozone. *J. Geophys. Res.* 111, D08301.
- Stuber, N., Ponater, M., Sausen, R., 2005. Why radiative forcing might fail as a predictor of climate change. *Clim. Dyn.* 24, 497–510.
- Stuber, N., Sausen, R., Ponater, M., 2001. Stratospheric adjusted radiative forcing calculations in a comprehensive climate model. *Theor. Appl. Climatol.* 68, 125–135.
- Toumi, R., Haigh, J., Law, K., 1996. A tropospheric ozone-lightning climate feedback. *Geophys. Res. Lett.* 23 (9), 1037–1040.
- Unger, N., Shindell, D., Koch, D., Streets, D.G., 2008. Air pollution radiative forcing from specific emissions sectors at 2030. *J. Geophys. Res.* 113 (D02306).
- Uno, I., He, Y., Ohara, T., Yamaji, K., Kurokawa, J.-I., et al., 2007. Systematic analysis of interannual and seasonal variations of model-simulated tropospheric NO_2 in Asia and comparison with GOME-satellite data. *Atmos. Chem. Phys.* 7 (6), 1671–1681.
- Wang, Z., Chien, C.-J., Tonnesen, G., 2009. Development of a tagged species source apportionment algorithm to characterize three-dimensional transport and transformation of precursors and secondary pollutants. *J. Geophys. Res.* 114, D21206.
- WMO, 2003. (world Meteorological Organization) Scientific Assessment of Ozone Depletion: 2002, Global Research and Monitoring Project-report 47.